SOFT SWITCHING FOUR QUADRANT DC-LINK INVERTER GENERATING SINUSOIDAL WAVEFORMS

Byeong O. Woo

GoldStar Industrial System Co. Ltd.
533 Hogye-dong, Anyang-shi
Kyongki-do 430-080, KOREA
(FAX : 82-343-53-6263)

Gyu H. Cho

Dept. of Electrical Eng., KAIST
373-1 Kusong-dong, Yusong-gu
Taejon 305-701, KOREA
(FAX : 82-42-829-3410)

ABSTRACT

A new soft switching converter topology for high frequency AC/DC/AC power conversion is proposed, which synthesizes the sinusoidal output voltages and results in the dramatic reduction of acoustic noise. The new converter achieves soft switching without increasing voltage or current ratings of devices and has capability of high frequency and four quadrant operation. The high frequency operation by soft switching provides several advantages such as high power density, low EMI and high dynamic performance. The voltage stresses and the current stresses in this converter are limited to the supply voltage and the link current respectively by the operation of current freewheeling circuit, and thus the VA ratings of devices are reduced to those of the hard switched inverters.

Operational principles, analyses and control method of the proposed converter are presented. Simulation results are also shown to verify the operational principle.

INTRODUCTION

Many soft switching converters have received considerable attention to replace the conventional hard-switched converters. The increase of a switching frequency resulted from eliminating switching losses by soft switching shows distinctive advantages such as high power density, low EMI, low acoustic noise and high dynamic performance. Resonant circuit adopted to achieve soft switching unfortunately always invokes substantial penalties such as higher VA ratings for devices and handing a multiple of the load power due to an increase of current and/or voltage. It has hampered high power converters with soft switching although many converter topologies are quite well suited to the power conversion in the low power range to be successful ones.

A lot of converter topologies[1-14] have been suggested and studied to apply soft switching technique to the high power conversion. The resonant pole inverter has the advantage of integrating the resonant component and the output filters. However the power range is limited due to high current stress and losses in devices and components. The auxiliary resonant commutated pole inverter[4] has the attractive features of soft switching without additional voltage and current stress in devices and low losses in additional passive elements. Unfortunately it requires twice device counts to be not cost effective compared to hard switched inverter. The actively clamped resonant dc-link inverter[2] requiring only one additional devices and limiting the device voltage stresses to 1.3-1.5Vs has been considered to be notable renewal in high power soft switching approach. However it has a harmonic component below the switching frequency and thus needs a higher switching frequency to obtain the same performance as the conventional PWM inverter because of a discrete pulse modulation.

An new converter topology which reduces the VA ratings of devices and has excellent output waveforms by inherent output filter capacitor was proposed[1]. The idea of providing a current freewheeling path in circuits for soft switching in order to limit an excessive current or voltage build-up is attractive. The insertion of current freewheeling circuit makes it possible to separate the main power flow interval from the resonant operation so that the VA ratings of devices are remarkably reduced. However the mode transition between the powering operation and the regenerative operation requires additional two switches except freewheeling switch in the link and it complicates the power circuits and converter control.

In this paper a new soft switching converter generating sinusoidal output voltages with only one additional switch is proposed which preserves the desired features of the previously proposed-converter[1]. The existence of a common mode between the powering operation and the regenerative operation simplifies the power circuit and alleviates the control complexity. The voltage and current stresses of devices are limited to the supply voltage and the link current respectively by the operation of a current freewheeling circuit. This converter is capable of four quadrant operation and dramatically reduces acoustic

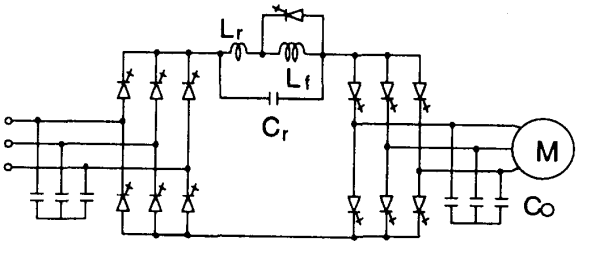

Fig. 1. Proposed converter configuration

0-7803-0695-3/92 $3.00

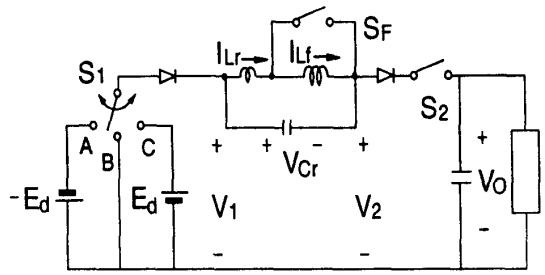

Fig. 2. Equivalent circuit

noise due to the sinusoidal output voltage. Operational principles, analyses and simulation results are presented in detail in this paper.

PROPOSED CONVERTER

The proposed converter is shown in Fig. 1. The front-end converter is controlled for its output to be one of among zero, maximum(E_d) and minimum($-E_d$) of line-to-line supply voltage by selecting the switches properly while maintaining the input power factor near unity. The inductor L_f is much larger than L_r to be approximated by a current source and the output filter capacitor C_o is also much larger than C_r to be approximated by a voltage source during one switching cycle. Since the main current flow on the link is always positive direction from the input to the output, turning-on of the upper switch among one of output inverter legs causes the corresponding phase voltage to increase, on the other hand, turning-on of the low part switch causes the phase voltage to decrease. Therefore it is possible to synthesize the wanted sinusoidal output voltage by properly selecting the inverter switch on every switching cycle. The operation modes directly depend on the polarity of the reflected voltage from the output capacitor to the link and are divided into powering operation(V_o>0) and regenerative one(V_o <0). The power flow is forward from the input line to the output capacitor during the powering operation and backward during the regenerative operation. Fig.2 shows the equivalent circuit of the proposed converter.

PRINCIPLE OF OPERATION

Fig. 3 shows the switch status and waveforms during the powering operation that consists of six modes, where the voltage increment of output capacitor during one switching cycle is neglected for the simplicity of explanation. Assume that the current of inductor L_f is $I_F(k)$ and freewheels through S_F and capacitor C_r is changed to $(E_d - V_o)$ while the current of inductor L_r is zero.

1) Mode P1 (t_1, t_2) : The inductor current $I_{Lr}(t)$ increases rapidly since the freewheeling switch conducts and the whole voltage across the link is applied to the inductor L_r. During this interval the inductor current and the capacitor voltage are given by

$$I_{Lf}(t) = I_F(k) \tag{1.a}$$

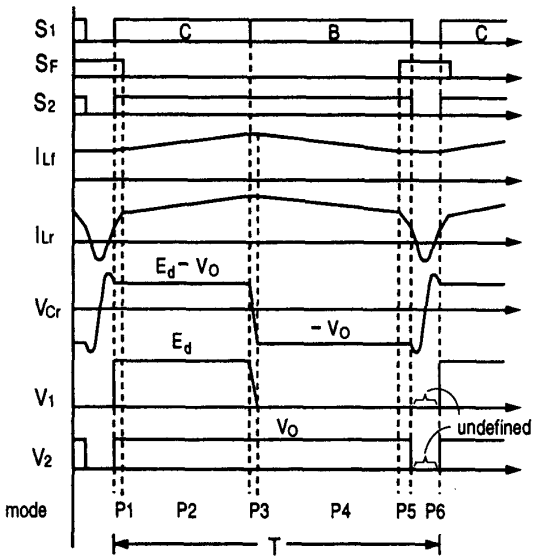

Fig. 3. Switch statuses and voltage and current waveforms for the equivalent circuit during powering operation

$$I_{Lr}(t) = \frac{1}{L_r}(E_d - V_o)t + I_{Lr}(t_1) \tag{1.b}$$

$$V_{Cr}(t) = E_d - V_o \tag{1.c}$$

After a while the resonant inductor current $I_{Lr}(t)$ is limited to the link current $I_{Lf}(t)$ and the freewheeling switch S_F is turned off under zero current.

2) Mode P2 (t_2, t_3) : Since the switch S_F is turned off, the resonant inductor L_r and the link inductor L_f effectively work in series. The current of series connected inductor increase slowly because of large inductance.
In this interval

$$I_{Lf}(t) = \frac{1}{(L_r + L_f)}(E_d - V_o)t + I_F(k) \tag{2.a}$$

$$I_{Lr}(t) = I_{Lf}(t) \tag{2.b}$$

$$V_{Cr} = E_d - V_o \tag{2.c}$$

Neglecting the voltage increment the equation (2.a) represents that the inductor current increase linearly during this interval. When the inductor current reaches the wanted value $I_F(k+1) + \Delta I$, this mode ends by turning-off the switch S_F.

3) Mode P3 (t_3, t_4) : The capacitor C_r is almost linearly discharged since this interval is short enough to neglect the inductor current variation.
The equation are given by

$$I_{Lf}(t) \cong I_F(k) + I_{Lf}(t_3) = \Delta I \tag{3.a}$$

$$I_{Lr}(t) = I_{Lf}(t) \tag{3.b}$$

$$V_{Cr}(t) \cong -\frac{1}{C_r}(I_F(k) + \Delta I)t + E_d - V_o \tag{3.c}$$

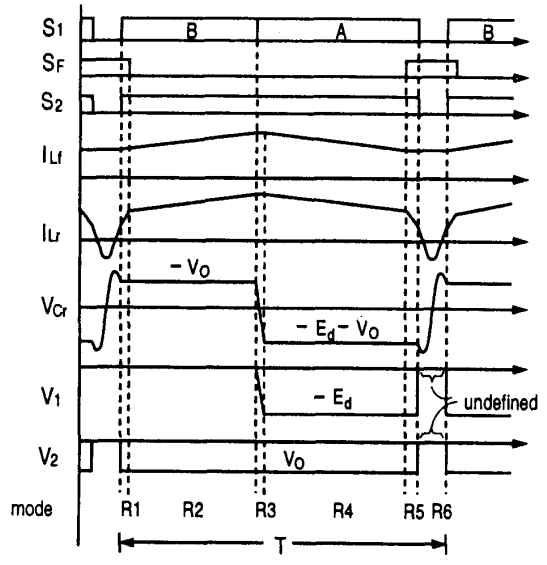

Fig. 4. Switch statuses and voltage and current waveforms for the equivalent circuit during regenerative operation

As soon as capacitor voltage reaches $-V_o$ the front-end switch S_1 conducts under zero voltage through point B.

4) Mode P4 (t_4, t_5) : The current of series connected inductor decreases almost linearly since the output capacitor voltage is reversely applied to the inductor in reverse direction.

Thus

$$I_{Lf}(t) = -\frac{1}{(L_s + L_r)} V_o t + I_{Lf}(t_4) \tag{4.a}$$

$$I_{Lr}(t) = I_{Lf}(t) \tag{4.b}$$

$$V_{Cr}(t) = -V_o \tag{4.c}$$

This mode ends by turning-on S_F when $I_{Lf}(t)$ is decreased to the wanted value $I_F(k+1)$ that is the freewheeling current during next commutation interval.

5) Mode P5 (t_5, t_6) : In this interval the inductor current $I_{Lf}(t)$ starts to freewheel through S_F. The current $I_{Lf}(t)$ decays abruptly since output capacitor voltage is reversely applied to inductor L_r.

The equations are given by.

$$I_{Lf}(t) = I_F(k+1) \tag{5.a}$$

$$I_{Lr}(t) = -\frac{1}{L_r} V_o t + I_{Lr}(t_5) \tag{5.b}$$

$$V_{Cr}(t) = -V_o \tag{5.c}$$

This mode ends when the inductor current $I_{Lf}(t)$ is reduced to I_{COM} defined as following;

$$I_{COM} = \frac{1}{Z_r}\sqrt{E_d^2 - V_o^2} \tag{5.d}$$

where $Z_r = \sqrt{\frac{L_r}{C_r}}$

6) Mode P6 (t_6, t_7) : Inductor current $I_{Lf}(t)$ continue to freewheel and the trapped energy to inductor L_r is transferred the capacitor by resonance.

$$I_{Lf}(t) = I_F(k+1) \tag{6.a}$$

$$I_{Lr}(t) = I_6 \sin \omega_r t + I_{Lr}(t_6) \cos \omega_r t \tag{6.b}$$

$$V_{Cr}(t) = \frac{1}{C_r \omega_r}(I_6 \cos \omega_r t - I_{Lr}(t_6) \sin \omega_r t) \tag{6.c}$$

where $I_6 = -\frac{V_o}{Z_r}$

When $I_{Lr}(t)$ becomes zero, the voltage $V_{Cr}(t)$ reaches its peak value.

From the energy conservation and equation (5.c) and (5.d), the peak value is given by

$$V_{Cr,peak} = \sqrt{V_{Cr}(t_6)^2 + \left(\frac{L_r}{C_r}\right) I_{Lr}(t_6)^2} \tag{7}$$
$$= E_d$$

After mode 6 ends, all states are the same as those of the beginning of mode1. Therefore, a next switching cycle can start again.

As mentioned above the powering and the regenerative operation are classified according to the direction of the power flow between the input line and output capacitors. In the regenerative operation the power flow is reversed from the output capacitor to the input line. The regenerative operation is similar to that of the powering operation except that the equivalent front-end converter switch is switched to B(during mode1 and mode2) and then A(during mode3 and mode4) in sequence. During the regenerative operation the switch status and waveforms are shown in Fig. 4 and analytical expressions are summarized in Appendix.

CHARACTERISTIC

The voltage stresses of the devices and components are limited to the maximum supply voltage and the current stress is always clamped to the link current. Therefore the VA ratings of this converter are very low compared with those of any other resonant link inverters. Sinusoidal voltages for both sides provide high quality waveforms to the input and to the load and result in lower harmonic current and lower acoustic noise in the motor drive system.

LINK CURRENT CONTROL

From the equation (2.a) and (4.a), the link current varies during mode2 and mode4 as followings,

$$\Delta_2 I = \frac{E_d - V_o}{L_r + L_f} \Delta t_2 \tag{8}$$

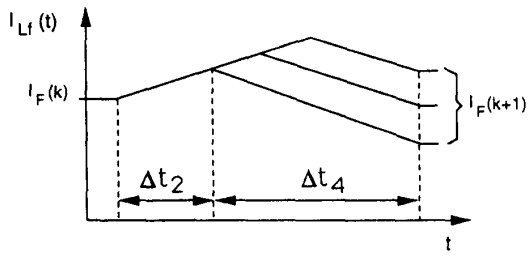

Fig. 5. Link current variation during one switching cycle

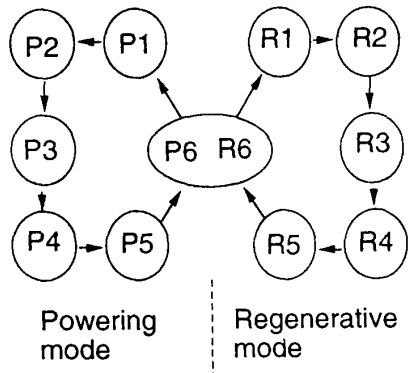

Fig. 6. Mode transition diagram

$$\Delta_4 I = -\frac{V_o}{L_r + L_f}\Delta t_4 \tag{9}$$

Since mode3 is short enough to neglect the current variation and the current freewheels during mode1, mode5 and mode6, the link current variation for one switching cycle is given by,

$$I_F(k+1) - I_F(k) \cong \frac{E_o - V_o}{L_r + L_f}\Delta t_2 - \frac{V_o}{L_r + L_f}\Delta t_4 \tag{10}$$

Where $I_F(k)$ and $I_F(k+1)$ represents the freewheeling current in k'th and (k+1)'th switching cycle. Fig.5 shows the current control method by the ratio of Δt_2 and Δt_4 under a constant switching cycle.

THREE PHASE CONFIGURATION

A. Mode Transition

The proposed converter synthesizes sinusoidal voltages at the output capacitor by impressing the high frequency link current cycle by cycle to the selected output capacitor. It should be noted that the selection of the inverter switches is done by observing the errors. Therefore, the reflected voltage(V_o) from the output capacitor to the link is varied cycle by cycle and its polarity also can be changed. Considering that the operation mode of powering and regenerative operation are directly dependent on the voltage polarity of an inverter input voltage, it is necessary to have mode transition capability between the powering and regenerative operations. Fortunately in this converter the

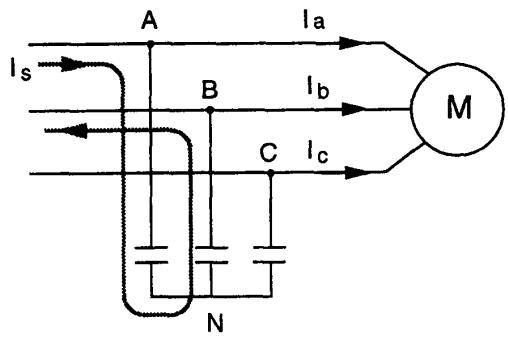

Fig. 7. Three phase configuration for output capacitor bank and load where phase A and B are compensated

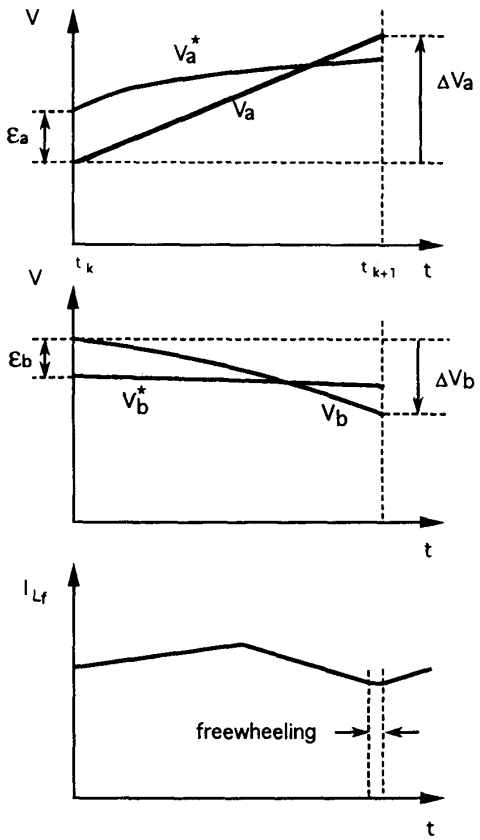

Fig. 8. Compensation process for phase A and B

powering and regenerative operation have a common mode(mode 6) as shown in Fig. 6. Thus it do not need any other action for a mode transition. By delivering or extracting the power in each individual high frequency cycle it is possible to synthesize a sinusoidal output voltage independently to the load condition.

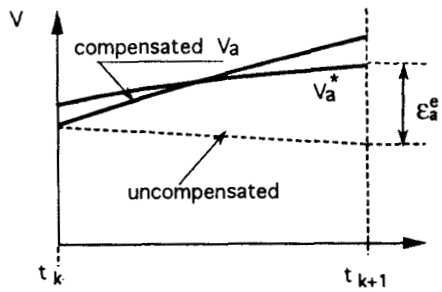

Fig. 9. Compensation process based on one step ahead errors calculation

B. Error Compensation with Present Data

To make an output capacitor voltage follow the sinusoidal references, phase switches conducting during next switching cycle should be determined at mode 6. Three errors between the reference voltage and the capacitor voltages are calculated.
Thus

$$V_a^* - V_a = \varepsilon_a$$
$$V_b^* - V_b = \varepsilon_b \qquad (11)$$
$$V_c^* - V_c = \varepsilon_c$$

and

$$\varepsilon_a + \varepsilon_b + \varepsilon_c = 0$$

The selection principle of phases compensated during next switching cycle are as followings : the phase having the largest error out of three phase is firstly chosen and then the phase having the larger error among the opposite polarity error is selected. The upper switch corresponding to a positive error phase and the lower switch of the phase with a negative error conduct to compensate both phase errors. Fig. 7 shows three phase configuration for output capacitor bank and load where phase A and B are compensated. Compensation process for phase A are shown in Fig. 8.

C. Error Compensation with Prediction

By measuring the load currents together with output voltages, it is sufficient to know the uncompensated output voltage without of the next state,

$$V_a(t_{k+1}) = V_a(t_k) + \frac{1}{C_o} I_a T$$
$$V_b(t_{k+1}) = V_b(t_k) + \frac{1}{C_o} I_b T \qquad (12)$$
$$V_c(t_{k+1}) = V_c(t_k) + \frac{1}{C_o} I_c T$$

Above equations show the calculation of a predicted output voltage for the next state. Since we know the estimated output voltage and the reference voltages, we can obtain the expected error quantities for the next state before the next switching occurs,

$$V_a^*(t_{k+1}) - V_a(t_k) = \varepsilon_a'$$
$$V_b^*(t_{k+1}) - V_b(t_k) = \varepsilon_b' \qquad (13)$$
$$V_c^*(t_{k+1}) - V_c(t_k) = \varepsilon_c'$$

Based on one step ahead errors instead of present values, we can also determine which phases should be chosen for the next state. Fig. 9 shows three phase reference voltages, the expected output voltage without compensation and the actual output voltages with compensation based on one ahead errors. It can be seen that the selection of phases compensated is based on error values at not $t = t_k$ but $t = t_{k+1}$. From simulations better results were obtained in this way.

SIMULATION RESULTS

The proposed converter is simulated to verify the operation. Input AC source voltage is $300V_{peak}$ and the parameters used for simulations are as followings ;

$L_r = 30\mu H$

$L_f = 1mH$

$C_r = 30nF$

$C_o = 30\mu F$

Simulation waveforms obtained with this converter are shown in Fig. 10. The simulation results are in good agreement with the expected waveforms as shown in Fig. 3 and Fig. 4. Fig. 11 shows the simulation results for the inverter output voltage waveforms when the command is abruptly changed. It can be seen that transient interval is short and a very fast response is obtained. As expected previously the simulation results show that the voltage stresses on all of the devices are almost equal to source voltage and the peak current stresses are limited to the link current.

CONCLUSION

A new high frequency dc-link converter generating sinusoidal waveforms for both input and output sides with soft switching capability is proposed and verified by the simulation. The proposed converter can operate on full four quadrants and provides several improved characteristics over the other resonant link inverter such as low VA ratings, low acoustic noise and low harmonic distortion. The voltage and current stresses are also low and always limited to the maximum of supply voltage and the link current respectively. The front-end converter can operate on almost unity power factor as well.
The features of the proposed converter can be summarized as follows :

* elimination of switching losses due to soft switching
* low VA ratings of devices
* four quadrant operation
* low harmonic on both input and output side

* capability of constant frequency operation
* simple power structure
* fast response and low acoustic noise
* four quadrant operation
* suitable for high power level

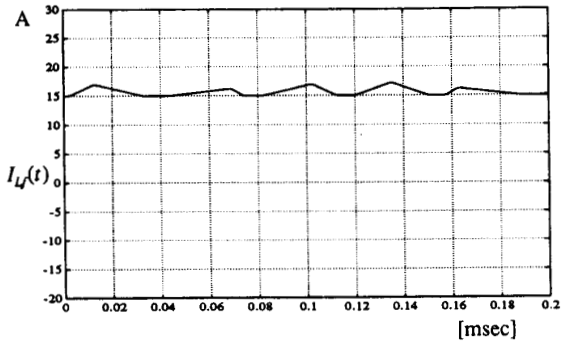

(a) link inductor current

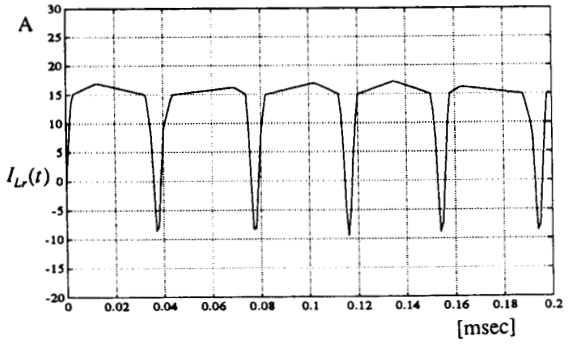

(b) resonant inductor current

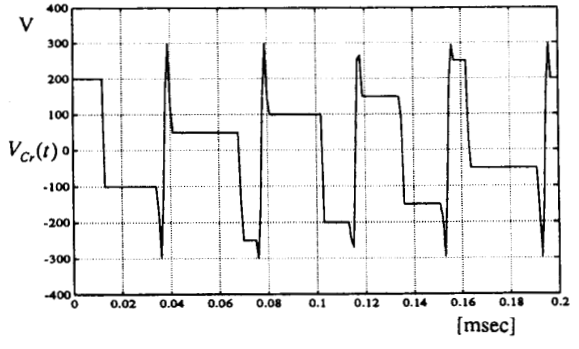

(c) resonant capacitor voltage

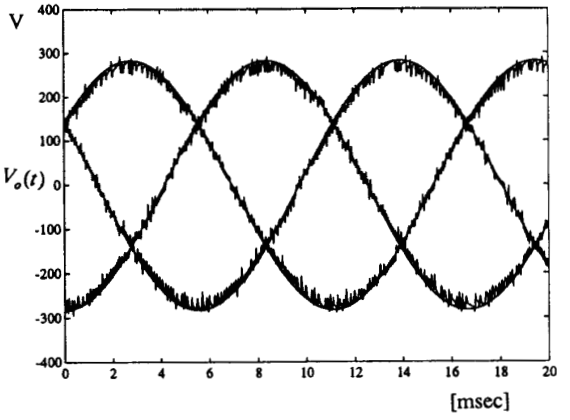

(d) output voltage

Fig. 10. Simulated waveforms

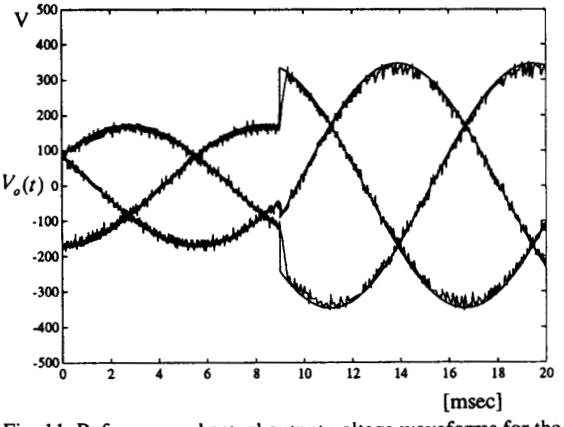

Fig. 11. Reference and actual output voltage waveforms for the change of output voltage references

REFERENCES

[1] B. O. Woo and G. H. Cho, "Soft switching AC/DC/AC converter with current freewheeling circuit", IEEE PESC Rec., pp. 31-38, 1991.

[2] D. M. Divan and G. Skibinski, "Zero switching loss inverters for high power applications", IEEE Trans. Ind. Appl., vol.25, no.4, pp. 634-643,July/August. 1989.

[3] Y. Murai and T. A. Lipo, "High frequency series resonant dc link power conversion", IEEE IAS Rec., pp. 772-779, 1988.

[4] R. W. De Doncker and J. P. Lyons, "The auxiliary resonant commutated converter", IEEE IAS Rec., pp. 1228-1235, 1990.

[5] Y. Murai et al, "Current pulse control of high frequency series resonant dc link power converter", IEEE IAS Rec., pp. 1021-1036, 1989.

[6] Jih-Sheng Lai and B. K. Bose, "High frequency quasi-resonant dc voltage notching inverter for ac motor drives", IEEE IAS Rec., pp. 1203-1217, 1990.
[7] B. O. Woo, I. D. Kim and G. H. Cho, "Zero voltage switching AC/DC/AC converter using modified high frequency dc-link", IEEE IAS Rec., pp. 1243-1250, 1990.
[8] S. S. Park and G. H. Cho, "A current regulated pulse width modulation method with new series resonant inverter", IEEE IAS Rec., pp. 1045-1051, 1989.
[9] E. C. Nho and G. H. Cho, "A new high performance zero-voltage zero-current mixed mode switch DC/DC converter", IEEE PESC, pp. 902-908, 1989.
[10] I. D. Kim and G. H. Cho, "New bilateral zero-voltage switching AC/AC converter using high frequency partial resonant link", IEEE IECON Rec., pp. 857-861, 1990.
[11] D. M. Divan, "Resonant dc link converter - a new concept in static power conversion", IEEE IAS Rec., pp. 648-656, 1986.
[12] G. Venkataramknan and D. M. Divan, "Pulse width modulation with resonant dc link converters", IEEE IAS Rec., pp. 984-990, 1990.
[13] D. I. A. Mertens and D. M. Divan, "A high frequency resonant dc link inverter using IGBT's", IEE of Japan IPEC Rec., pp. 152-160, 1990.
[14] S. K. Sul and T. A. Lipo, "Field oriented control of an induction machine in a high frequency link power system", IEEE PESC Rec., pp. 1084-1090, 1988.

APPENDIX

Analytical expressions for the link current, the resonant inductor current and resonant capacitor voltage of the six modes during regenerative operation are given as follows. (V_o<0)

1) Mode R1 : (t_1 , t_2)

$$I_{Lf}(t) = I_F(k) \tag{A.1a}$$

$$I_{Lr}(t) = -\frac{V_o}{L_r}t + I_{Lr}(t_1) \tag{A.1b}$$

$$V_{Cr}(t) = -V_o \tag{A.1c}$$

2) Mode R2 : (t_2 , t_3)

$$I_{Lf}(t) = \frac{V_o}{L_f + L_r}t + I_F(k) \tag{A.2a}$$

$$I_{Lr}(t) = I_{Lf}(t) \tag{A.2b}$$

$$V_{Cr}(t) = -V_o \tag{A.2c}$$

3) Mode R3 : (t_3 , t_4)

$$I_{Lf}(t) \equiv I_{Lf}(t_3) \tag{A.3a}$$

$$I_{Lr}(t) = I_{Lf}(t) \tag{A.3b}$$

$$V_{Cr}(t) \equiv -\frac{1}{Co}I_{Lf}(t_3)t + V_o \tag{A.3c}$$

4) Mode R4 : (t_4 , t_5)

$$I_{Lf}(t) = -\frac{(E_d - V_o)}{(L_f + L_r)}t + I_{Lf}(t_4) \tag{A.4a}$$

$$I_{Lr}(t) = I_{Lf}(t) \tag{A.4b}$$

$$V_{Cr}(t) = -E_d - V_o \tag{A.4c}$$

5) Mode R5 : (t_5 , t_6)

$$I_{Lf}(t) = I_F(k+1) \tag{A.5a}$$

$$I_{Lr}(t) = -\frac{(E_d + V_o)}{L_r}t + I_f(k+1) \tag{A.5b}$$

$$V_{Cr}(t) = -E_d - V_o \tag{A.5c}$$

6) Mode R6 : (t_6 , t_7)

$$I_{Lf}(t) = I_F(k+1) \tag{A.6a}$$

$$I_{Lr}(t) = I_6 \sin\omega_r t + I_{Lr}(t_6)\cos\omega_r t \tag{A.6b}$$

$$V_{Cr}(t) = \frac{1}{C_r\omega_r}(I_6\cos\omega_r t - I_{Lr}(t_6)\sin\omega_r t) \tag{A.6c}$$

where $I_6 = -\frac{(E_d + V_o)}{Z_r}$